



# Study on Factors Affecting Remote Sensing Ecological Quality Combined with Sentinel-2

Qiang Fan <sup>1</sup>, Yue Shi <sup>1</sup>, Xiaonan Song <sup>1</sup> and Nan Cong <sup>2,\*</sup>

<sup>1</sup> School of Geomatics, Liaoning Technical University, Fuxin 123000, China; fanqiang@lntu.edu.cn (Q.F.); 47221050@stu.lntu.edu.cn (Y.S.); 472020771@stu.lntu.edu.cn (X.S.)

<sup>2</sup> Lhasa Plateau Ecosystem Research Station, Institute of Geographic Sciences and Natural Resources Research, Chinese Academy of Sciences, Beijing 100101, China

\* Correspondence: congnan@igsnr.ac.cn

**Abstract:** Reasonable allocation of urban resources can effectively control changes in ecological quality. This study used Sentinel-2 images, taking urban functional areas as the dividing scale, and combined spatial analysis, statistics, and other relevant methods to explore the factors influencing remote sensing ecological quality in Puxi, Shanghai, China. Landsat-8 and high-resolution Sentinel-2 data fusion achieved more refined remote sensing ecological index (RSEI) distribution data, which is of great significance for ecological quality exploration in small areas; the degree of influence of the selected research factors on the RSEI was spectral index > building > social perception > terrain. The R-value of the soil-adjusted vegetation index (SAVI) was 0.970, and it exerted the strongest influence. The R-value of the average building height was 0.103, indicating that it had the weakest influence. The interactions among the selected factors were mainly two-factor and nonlinear enhancements. Most factor combinations exhibited two-factor enhancement. There were six groups of factor combinations for nonlinear enhancement, of which five were related to the average building height. The results of the present study provide a reference for multi-path ecological quality control in small-area regions.

**Keywords:** remote sensing ecological quality; GEO-detector; influence factor; urban functional area; Sentinel-2



**Citation:** Fan, Q.; Shi, Y.; Song, X.; Cong, N. Study on Factors Affecting Remote Sensing Ecological Quality Combined with Sentinel-2. *Remote Sens.* **2023**, *15*, 2156. <https://doi.org/10.3390/rs15082156>

Academic Editor: Monica Rivas Casado

Received: 13 February 2023

Revised: 12 April 2023

Accepted: 14 April 2023

Published: 19 April 2023



**Copyright:** © 2023 by the authors. Licensee MDPI, Basel, Switzerland. This article is an open access article distributed under the terms and conditions of the Creative Commons Attribution (CC BY) license (<https://creativecommons.org/licenses/by/4.0/>).

## 1. Introduction

In the wake of rapid global economic development, there has been significant economic stratification between cities and villages. Improved employment and living environments have attracted many rural residents to cities. Owing to the rapid increase in the urban labor force, social and economic development has also been rapid; however, urban environmental challenges, such as excessive exhaust emissions, serious land loss, and severe air pollution, have ensued, resulting in ecological challenges, the effects of which are experienced far beyond urban boundaries [1]. The ecological environment has attracted considerable attention in medium-sized and large cities [2–5], and the effective control of regional ecological environmental quality has become a major research topic [6–8].

The rational assessment of ecological environmental quality has become a system after years of development. In 2003, researchers developed a conceptual framework of environmental quality [9], which provides guidance for the assessment of urban ecological environment quality. Moreover, ecological quality assessment methods, such as the ecological index (EI) [10], invest [11], and the remote sensing ecological index (RSEI) [12], are gradually being recognized by the research community. Among them, the RSEI is a method of assessing regional ecological quality based on full remote sensing. Given the convenience of the data acquisition, intuitive effect, and lower manpower and financial costs associated with this method, it is commonly used in regional ecological environment quality regulation research.

The precise control of the factors influencing ecological quality can effectively prevent detrimental changes in ecological quality. Previous research has used MODIS and Landsat series images to explore factors influencing the RSEI, ranging from climate, human disturbance, land use, soil, and urbanization, among others [13–17]. However, owing to human activities, ecosystems, climate change, and other regional differences, the methods of quality control of ecological environments over large areas are not fully applicable to small areas. We suggest that high-resolution data are needed to explore different influencing factors in ecological environments for small areas. The Sentinel-2 dataset has a spatial resolution of 10 m and can provide higher-resolution textural information on ground objects compared with the MODIS and Landsat series datasets. Using Sentinel-2 data to explore the factors influencing the RSEI can gradually improve the comprehensive management of ecological quality.

The emergence of urban functional zoning is convenient for urban ecological studies, including the mechanism of change in thermal environments under urban functional zoning [18], the precipitation-runoff characteristics of urban commercial and non-commercial zones [19], and carbon emission estimation using multi-source data in urban functional zones [20]. However, few studies have taken the urban functional area as the dividing scale of the RSEI and explored its influencing factors. In summary, urban remote sensing ecological quality control in small areas should be explored further.

Therefore, the present study utilized high-resolution Sentinel-2 images to analyze the factors influencing the regional RSEI by synthesizing four major factors—the terrain, architecture, social perception, and spectral index—to provide a reference for precisely regulating ecological quality.

## 2. Data and Methods

### 2.1. Research Area

Shanghai (Figure 1) is an important economic, financial, and technological innovation center in China [21,22], located at 120°52′–122°12′E and 30°40′–31°53′N. Seven districts from Puxi are located in the central urban area west of the Huangpu River, including Putuo District, Xuhui District, Changning District, Yangpu District, Hongkou District, Jingan District, and Huangpu District. The study area is located on the flat Yangtze River Delta Plain; the water net is dense. The hills are scattered in the southwest and have an average altitude of approximately 4 m. Puxi has a subtropical monsoon climate with four distinct seasons, full sunshine, long summers, and hot and dry weather. Owing to many human activities and frequent land cover replacement, it is difficult to control the ecological quality of the Puxi region. However, the rational layout of urban resources could improve the urban ecological quality.

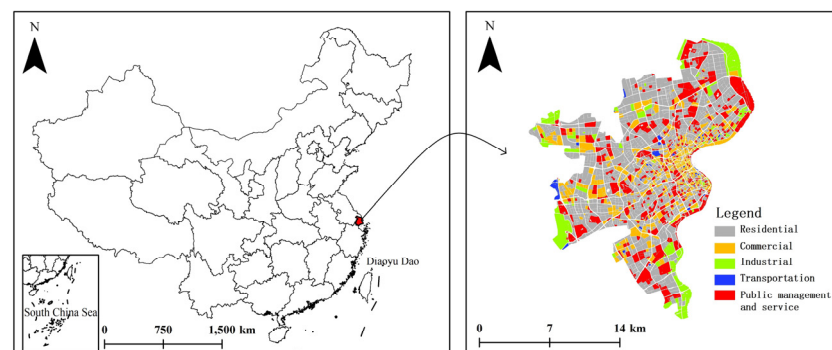


Figure 1. Location map of the study area.

### 2.2. Research Data

The Sentinel-2 dataset used in the present study was obtained from the Copernicus Open Access Center (<https://scihub.copernicus.eu/dhus/#/home>; image time is 16 August 2020). The Landsat-8 TIRS data were derived from the geospatial data cloud

(<https://www.gscloud.cn/>; image time is 16 August 2020). The Point of Interest (POI) data were obtained from Baidu Map (<https://lbsyun.baidu.com/>; accessed on 2020). The building data were also sourced from Baidu Map data and were provided by Shuijingzhu (<http://www.rivermap.cn/> (accessed on 2021)); they included the building height in the attribute table. The data on urban functional areas were derived from EULUC-China data, which are refined functional area partition data completed by Gong et al. [23]. The Sentinel-2 data belong to the S2B satellite, and the product level is L1C. This level of data is geometrically refined, but radiometric calibration and atmospheric correction have not been carried out. Therefore, Sen2cor and SNAP were required for data preprocessing. Sen2cor mainly completes radiometric calibration and atmospheric correction, while SNAP mainly completes format conversion and generates IMG data that can be directly read by ENVI. The Landsat-8 data were resampled to 10 m resolution using ENVI. The POI and building data were cleaned, screened, and inspected.

### 2.3. Research Methods

Sentinel 2 images and Landsat-8 data were selected to extract the RSEI. The Pearson correlation coefficient and GEO-detector were combined to mine the factors influencing the RSEI. The main procedure is illustrated in Figure 2.

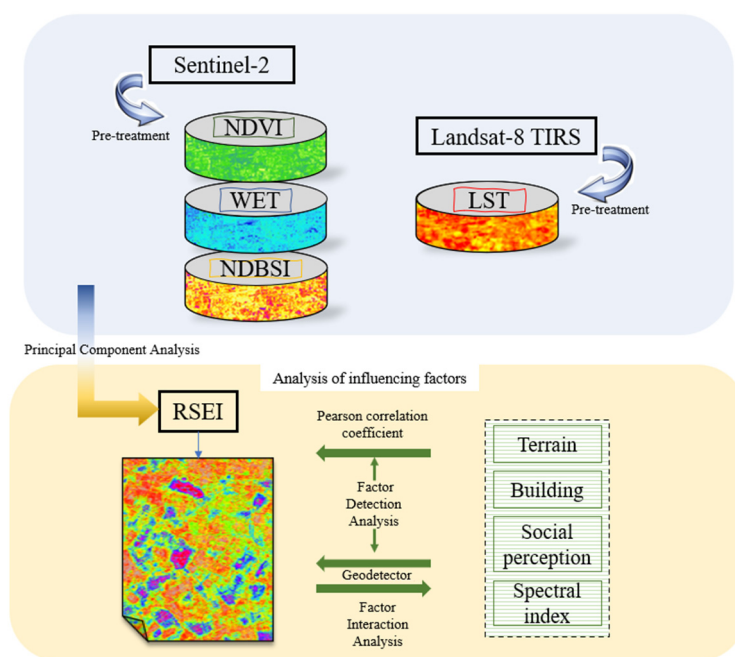


**Figure 2.** The roadmap of research.

#### 2.3.1. Remote Sensing Ecological Quality

The RSEI was used as a remote sensing ecological quality assessment method. This index integrates greenness, dryness, humidity, and heat, as follows:

$$\text{RSEI} = f(\text{NDVI}, \text{WET}, \text{NDBSI}, \text{LST}), \quad (1)$$

where the RSEI is the remote sensing ecological index, the normalized difference vegetation index (NDVI) is the greenness index, WET is the wetness index, the normalized difference bare soil index (NDBSI) is the dryness index, and the land surface temperature (LST) is the heat index. The NDVI is a spectral index [24] proposed to represent regional vegetation distribution. The greenness index selected by the RSEI was constructed using the NDVI. The K–T transformation is fixed based on the physical characteristics of the images. Several main components of the brightness, greenness, and wetness indices were obtained after transformation. The humidity index was expressed by the wetness component after the

Tasseled Cap Transformation [25]. As bare soil and buildings can comprehensively reflect the degree of “drying” of the ecological environment quality, the dryness index consisted of the mean values of the bare soil index (SI) and building index (IBI) [12]. The thermal index was the land surface temperature [26] inverted using the radiation equation method. As Sentinel-2 has high data resolution, the calculated land surface temperature data were resampled to a resolution of 10 m, and principal component analysis was performed.

### 2.3.2. Pearson Correlation Coefficient

In this study, the Pearson correlation coefficient was used to explore the degree of correlation between the influencing factors and the RSEI. The values were between  $-1$  and  $1$ , where zero indicates no relationship or correlation between the two factors,  $>0$  denotes a positive correlation between the two variables, and  $<0$  denotes a negative correlation between the two variables [27,28].

$$R = \frac{\sum_{i=1}^n (x_i - \bar{x})(y_i - \bar{y})}{\sqrt{\sum_{i=1}^n (x_i - \bar{x})^2} \sqrt{\sum_{i=1}^n (y_i - \bar{y})^2}}, \quad (2)$$

where  $R$  is the value of the correlation coefficient, whose value range is  $[-1, 1]$ ,  $x_i$  and  $y_i$  are the values of the variables,  $\bar{x}$  and  $\bar{y}$  are the average values of the variables, and  $n$  is the number of variables.

### 2.3.3. GEO-Detector

GEO-detector is a statistical method used to evaluate the factors influencing variables; it is used to explore spatial differentiation. There are four types of GEO-detectors. The factor detector detects the spatial differentiation of variable and the interpretation degree of factors to variables [29,30]. The  $q$  value is used to measure the influence of the factors, and the calculation formula is:

$$q = 1 - \frac{\sum_{h=1}^L N_h \sigma_h^2}{M \sigma^2} = 1 - \frac{SSW}{SST}, \quad (3)$$

where  $h = 1, \dots, L$  are the partitions of the variables  $Y$  and factors  $X$ ;  $N_h$  and  $M$  are the number of units in the area  $h$  and the whole area, respectively;  $\sigma_h^2$  and  $\sigma^2$  are the variance of the region  $h$  and the  $Y$  value of the whole region; and  $SSW$  and  $SST$  are the sum of the intra-area variance and the total variance of the whole area, respectively. The calculations yield a value of  $q$  ranging between 0 and 1.

The interaction detector mainly identifies the interaction between multiple independent and dependent variables, that is, it identifies whether the interaction of  $X_1$  and  $X_2$  will have an enhanced or weakened impact on variables, but the results may show that the independent variables are independent of the dependent variables. The detector calculates the values of  $q(X_1)$ ,  $q(X_2)$ , and  $q(X_1 \cap X_2)$  and compares the three values. The calculation primarily combines the data processing method proposed by Wang et al. [31,32].

## 3. Results and Analysis

### 3.1. Spatial Distribution of Remote Sensing Ecological Quality

Figure 3 shows the RSEI calculation results for the Landsat-8 and Sentinel-2 data. The RSEI calculated using the Sentinel-2 data has a similar spatial distribution as that calculated using the Landsat-8 data, but the spatial distribution of Sentinel-2 is more detailed. Based on the distribution pattern of the RSEI, areas with good ecological quality are scattered and distributed in green areas (e.g., parks, scenic spots, etc.). In addition, roadside trees and green belt areas alongside roads show good ecological quality distribution trends. The areas with poor ecological quality are concentrated on impervious surfaces, such as dense buildings and wide roads in urban centers. We tested the spatial autocorrelation of the RSEI values in different functional areas and determined that the value of Moran's  $I$  was 0.39, and the  $Z$  scores all exceeded the critical value of 1.96 at the 0.01 confidence level. This

confirms a significant spatial positive correlation, indicating that the RSEI values are not independent in space and have always been in a spatial agglomeration state.

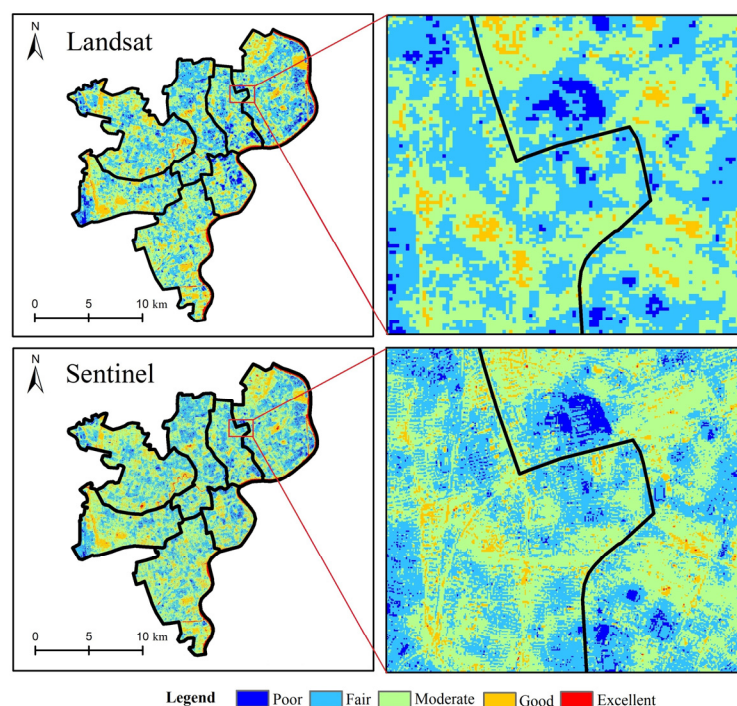


**Figure 3.** Detailed comparison of RSEI across the different datasets.

Table 1 shows the average values of the RSEI and the four indices in seven districts in Puxi. Given the high level of development in the seven districts, buildings generally occupy most of the space. Therefore, the regional heat feedback is roughly the same, the heat generated by ground features is approximate, and the LST values are not significantly different. The NDBSI values show positive and negative differences, indicating that the dryness index in the seven districts in Puxi is influenced by the surface cover. The dryness degree of Huangpu is the highest because of the high economic development. Based on the actual situation in the study area, 10 m resolution data can well distinguish the green plant distribution, and the overall NDVI value of the study area is low. Moreover, the overall fluctuation in the WET index is low. The study area is located close to the sea, and the combined action of high temperatures and sea winds in the summer and the water vapor emitted by green plants influence the WET values to a certain extent.

**Table 1.** Mean of the four indicators in the research area.

Administrative Division	LST (°C)	NDBSI	NDVI	WET	RSEI
Huangpu	39.327	0.036	0.210	−0.025	0.522
Xuhui	39.223	−0.010	0.309	−0.033	0.514
Changning	39.520	−0.023	0.357	−0.043	0.530
Jingan	40.623	0.018	0.273	−0.036	0.580
Putuo	39.795	−0.012	0.324	−0.039	0.535
Hongkou	40.136	0.010	0.274	−0.031	0.559
Yangpu	39.455	−0.001	0.287	−0.033	0.532

### 3.2. Factors Influencing Remote Sensing Ecological Quality

In recent years, research on the factors influencing the urban ecological environment, which mainly include buildings [33,34], land use [35], and local climate zones [36,37], has increased. The present study drew on previously identified factors and combined them

with the unique natural and anthropogenic characteristics of the study area. A total of 12 influencing factors (Table 2), based on four aspects (terrain factors, building factors, social perception factors, and spectral index factors), were used to explore the factors influencing the RSEI in seven Puxi districts. The Pearson correlation coefficient and GEO-detector were combined to analyze factor detection and interaction.

**Table 2.** Factors influencing remote sensing ecological quality.

Factor Type	Code	Factor
Terrain factors	X <sub>1</sub>	DEM
	X <sub>2</sub>	Slope
Building factors	X <sub>3</sub>	Building coverage
	X <sub>4</sub>	Density of building patches
	X <sub>5</sub>	Average building height
	X <sub>6</sub>	Space congestion
Social perception factors	X <sub>7</sub>	Dining distribution density
	X <sub>8</sub>	Distribution density of public land
	X <sub>9</sub>	Shopping distribution density
Spectral index factors	X <sub>10</sub>	SAVI
	X <sub>11</sub>	NDBI
	X <sub>12</sub>	MNDWI

### 3.2.1. Factor Detection Analysis

In the present study, the Pearson correlation coefficient and factor detector part of the GEO-detector were used to analyze the influencing factors. In combining the results in Table 3, the explanatory force of each factor on the RSEI was  $X_{10} > X_{12} > X_{11} > X_3 > X_6 > X_4 > X_9 > X_8 > X_7 > X_1 > X_2 > X_5$ . In combining the Pearson correlation coefficients (Figure 4), the digital elevation model (DEM), slope, average building height, and SAVI were observed to be positively correlated with the RSEI ( $p < 0.001$ ), while the building cover, building patch density, space congestion, food and beverage distribution density, public land distribution density, shopping place distribution density, NDBI, and MNDWI were negatively correlated with the RSEI ( $p < 0.001$ ).

**Table 3.** Factor detection analysis results. (The meanings of different indicators are shown in Table 2).

Factor	X <sub>1</sub>	X <sub>2</sub>	X <sub>3</sub>	X <sub>4</sub>	X <sub>5</sub>	X <sub>6</sub>
q	0.124	0.057	0.304	0.148	0.033	0.150
p Value	<0.001	<0.001	<0.001	<0.001	<0.001	<0.001
Factor	X <sub>7</sub>	X <sub>8</sub>	X <sub>9</sub>	X <sub>10</sub>	X <sub>11</sub>	X <sub>12</sub>
q	0.128	0.130	0.133	0.881	0.690	0.758
p Value	<0.001	<0.001	<0.001	<0.001	<0.001	<0.001

Overall, the spectral index factor had the strongest influence on the RSEI, followed by building, social perception, and terrain. The entirety of Shanghai is in the plain area of the Yangtze River Delta. Owing to the high proportion of buildings in the study area and minimal topographic fluctuation, the gradient changes only slightly, and topographic factors have little effect on the RSEI. These results are similar to those reported by Cui et al. [38]. POI data, as a specific representation of each geographical element, have been favored by many scholars in recent years. In this study, the distribution density was considered an influencing factor of the RSEI. As the main urban area of Shanghai, the shopping, catering, and public facilities in the seven Puxi districts are highly developed. The distribution density has an inhibitory effect on the RSEI. There are few vegetation and water areas where public activities are frequent, and many types of buildings have

adverse effects on the ecological quality. Few studies have examined the influence of this social perception factor on the RSEI. Among the building factors, the building cover had a significant negative impact on the RSEI. This interaction occurs not only in the seven districts of Puxi but also in most areas with high building cover. The impact of other building factors on the RSEI was relatively low, of which the impact of the average building height was the weakest but still passed the significance test, indicating that the impact of this factor cannot be ignored. The spectral exponential factors play a significant role in the RSEI. As the NDVI is one of the components of the RSEI, the SAVI was selected for further exploration. The results show that the soil-adjusted vegetation index represented by the SAVI has an important influence on the RSEI, with a 0.97 Pearson correlation coefficient and a positive promotion. Among the other spectral index factors, the building index represented by the NDBI had an inhibitory effect on the RSEI. The MNDWI also exerted a strong inhibitory effect on the RSEI. This is mainly related to the high building cover of the study area. The water surface area inside the study area is small, and remote sensing images have poor detection ability for small areas of water surface between buildings. Therefore, the negative effects of the RSEI are not alleviated.

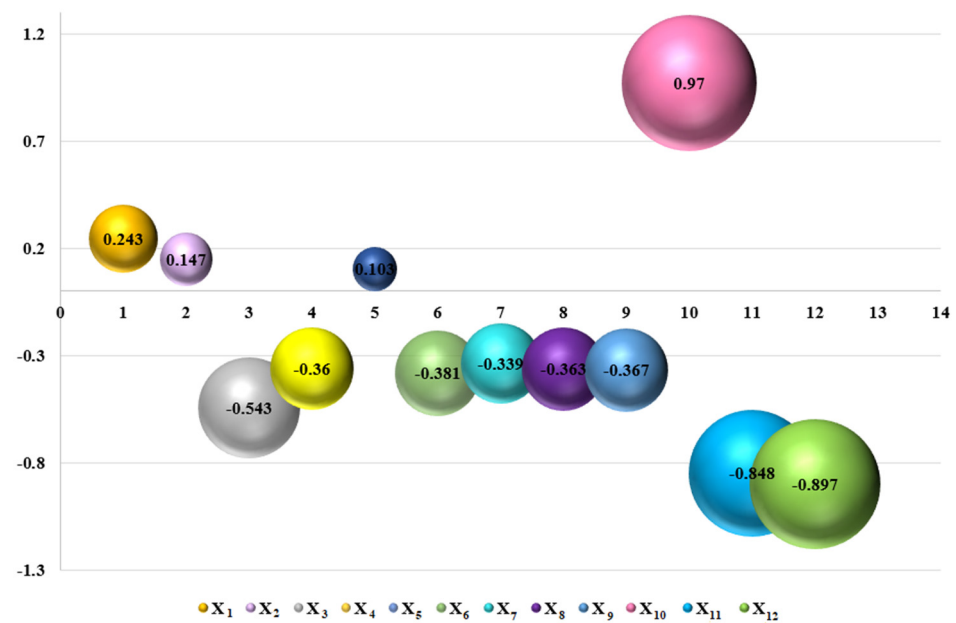


**Figure 4.** Pearson correlation coefficient results ( $X_1$  to  $X_{12}$  passed the significance test, ( $p < 0.001$ ); the meanings of different indicators are listed in Table 2).

### 3.2.2. Factor Interaction Analysis

Figure 5 presents the results of the two-factor interaction. The interaction between the selected factors and the RSEI showed two-factor or nonlinear enhancement, with no independent or weakening effects. Two-factor enhancement accounted for a large proportion. Nonlinear enhancement mainly occurred in  $X_2 \cap X_5$ ,  $X_1 \cap X_5$ ,  $X_1 \cap X_4$ ,  $X_7 \cap X_5$ ,  $X_8 \cap X_5$ , and  $X_9 \cap X_5$ . Except for the nonlinear enhancement between the DEM and building patch density, the other nonlinear enhancements were related to the average building height. This may be related to the weak impact of the average building height on the RSEI. The factors represented as two-factor enhancements indicated that the combined action of two factors had the most significant influence on the RSEI.

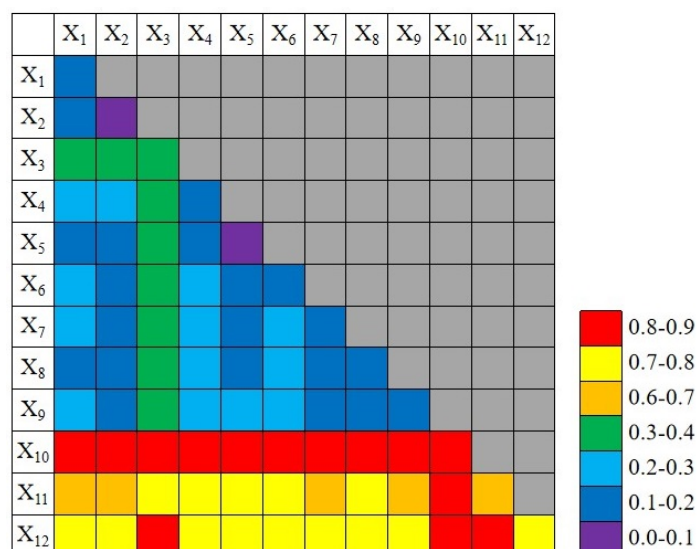


**Figure 5.** Factor interaction results (The meanings of different indicators are shown in Table 2).

The interaction between the SAVI and other factors had a promotional effect on the RSEI, in which the interaction enhancement of the SAVI∩average building height and SAVI∩space congestion was the highest, indicating that the positive effects of vegetation and reverse effects of buildings play a key driving role in the change in the RSEI. However, the high interaction between the SAVI and building factors was not the highest among the factor combinations. The highest value was for SAVI∩MNDWI, followed by SAVI∩NDBI, which shows that the spectral index has an important influence on the RSEI.

#### 4. Discussion

##### 4.1. Optimizing Urban RSEI

The factors influencing the RSEI identified in the present study include the terrain, buildings, social perception, and spectral index. The factors influencing the RSEI were explored in an extremely developed, small urban area. The building and social perception factors considered in the present study have seldom been mentioned in previous studies. A study of the correlation between these two types of factors and the RSEI can provide a reference for precisely adjusting the RSEI and considering the ecological quality during the development of modern cities.

Previous studies have reported various findings on the factors influencing the RSEI in different regions: the influence of human factors on the RSEI is increasing gradually in the Jing-Jin-Ji urban agglomeration [39]; the effect of the gross domestic product on the RSEI of the Loess Plateau is increasing gradually [40]; population and economy do not inhibit the RSEI in the Lhasa metropolitan area [41]; and the RSEI and the composition index of urban agglomeration on the northern slope of the Tianshan Mountains exhibit a certain relationship [42]. However, because of the small area, wide but complex vegetation distribution, and high building cover of the central urban setting, our study area differs significantly from those of the aforementioned studies. In particular, it is difficult to regulate the ecological quality of urban areas. Therefore, it is critical to optimize regional ecological quality from many aspects. Our multi-factor inquiry shows that RSEI optimization must rationalize the allocation of vegetation, buildings, and water areas, combined with evenly distributed social perceptive features, including but not limited to catering, shopping, and public land. Congestion, cover, and building height should also be considered in urban construction and planning. Moreover, the influence of topographic factors on the RSEI cannot be ignored.

#### 4.2. Limitations

This study only used the method of dividing urban functional areas to explore the factors influencing the RSEI in the seven districts of Puxi. The factors influencing the RSEI in administrative areas or grids should be continuously investigated. In addition, the factors influencing urban RSEI vary. Numerous factors that control changes in the RSEI have been observed in different cities owing to the geographical location and human, economic, and social factors. Future research will focus on these different factors.

#### 5. Conclusions

The ecological quality of small areas is affected by numerous factors. Reasonable adjustment of ecological quality is beneficial to human health and life quality. In the present study, high-resolution Sentinel-2 data were combined to explore the factors influencing the RSEI in the Puxi area based on four aspects: terrain, buildings, social perception, and spectral index. The main conclusions are as follows:

- (1) Owing to data resolution advantages, the RSEI spatial distribution data represented by Sentinel-2 are more detailed than those from the Landsat data, which is of more practical significance for the study of ecological quality in small areas.
- (2) The four factors selected in the study influenced the RSEI in the order of spectral index factor > building factor > social perception factor > terrain factor. The SAVI had the greatest influence and a significant positive correlation with the RSEI ( $R = 0.970$ ), whereas the average building height had the least influence and a significant positive correlation ( $R = 0.103$ ).
- (3) In the factor interaction analysis, only double factor enhancement and nonlinear enhancement existed among the selected factors. Most of the factor combinations exhibited two-factor enhancement; only six factor combinations exhibited nonlinear enhancement and five were related to the average building height. The interaction between the SAVI and each factor was strong, with the  $SAVI \cap MNDWI$  and  $SAVI \cap NDBI$  combinations having strong interactions with the RSEI. Furthermore, the  $SAVI \cap$  average building height and  $SAVI \cap$  space congestion exhibited strong interactions.

**Author Contributions:** Conceptualization, Q.F. and N.C.; Data curation, X.S. and Y.S.; Investigation, X.S. and Y.S.; Methodology, Q.F. and Y.S.; Validation, X.S.; Visualization, X.S.; Writing—original draft, N.C. and Y.S.; Writing—review and editing, Q.F., N.C., X.S. and Y.S. All authors have read and agreed to the published version of the manuscript.

**Funding:** This research was partially funded by a project supported by the Discipline Innovation Team of Liaoning Technical University (grant number LNTU20TD-06).

**Institutional Review Board Statement:** Not applicable.

**Informed Consent Statement:** Not applicable.

**Data Availability Statement:** Please refer to Chapter 2.2 of the article for detailed information on the sources of data used in this study.

**Conflicts of Interest:** The authors declare no conflict of interest.

#### References

1. McDonnell, M.J.; MacGregor-Fors, I. The ecological future of cities. *Science* **2016**, *352*, 936–938. [[CrossRef](#)] [[PubMed](#)]
2. Van Dijk, M.P.; Mingshun, Z. Sustainability indices as a tool for urban managers, evidence from four medium-sized Chinese cities. *Environ. Impact Asses.* **2005**, *25*, 667–688. [[CrossRef](#)]
3. Manes, F.; Marando, F.; Capotorti, G.; Blasi, C.; Salvatori, E.; Fusaro, L.; Ciancarella, L.; Mircea, M.; Marchetti, M.; Chirici, G. Regulating ecosystem services of forests in ten Italian metropolitan cities: Air quality improvement by  $PM_{10}$  and  $O_3$  removal. *Ecol. Indic.* **2016**, *67*, 425–440. [[CrossRef](#)]
4. Zhao, Z.; Sharifi, A.; Dong, X.; Shen, L.; He, B. Spatial variability and temporal heterogeneity of surface urban heat island patterns and the suitability of local climate zones for land surface temperature characterization. *Remote Sens.* **2021**, *13*, 4338. [[CrossRef](#)]

5. Chen, Y.; Yang, J.; Yu, W.; Ren, J.; Xiao, X.; Xia, J. Relationship between urban spatial form and seasonal land surface temperature under different grid scales. *Sustain. Cities Soc.* **2023**, *89*, 104374. [[CrossRef](#)]
6. McKinley, D.C.; Miller-Rushing, A.J.; Ballard, H.L.; Bonney, R.; Brown, H.; Cook-Patton, S.C.; Evans, D.M.; French, R.A.; Parrish, J.K.; Phillips, T.B. Citizen science can improve conservation science, natural resource management, and environmental protection. *Biol. Conserv.* **2017**, *208*, 15–28. [[CrossRef](#)]
7. Lihua, W.; Tianshu, M.; Yuanchao, B.; Sijia, L.; Zhaoqiang, Y. Improvement of regional environmental quality: Government environmental governance and public participation. *Sci. Total. Environ.* **2020**, *717*, 137265.
8. Guo, B.; Fang, Y.; Jin, X. Monitoring the effects of land consolidation on the ecological environmental quality based on remote sensing: A case study of Chaohu Lake Basin, China. *Land Use Policy* **2020**, *95*, 104569. [[CrossRef](#)]
9. Van Kamp, I.; Leidelmeijer, K.; Marsman, G.; De Hollander, A. Urban environmental quality and human well-being: Towards a conceptual framework and demarcation of concepts; a literature study. *Landsc. Urban. Plan.* **2003**, *65*, 5–18. [[CrossRef](#)]
10. Muthu, S.S.; Li, Y.; Hu, J.; Mok, P.Y. Quantification of environmental impact and ecological sustainability for textile fibres. *Ecol. Indic.* **2012**, *13*, 66–74. [[CrossRef](#)]
11. Zhu, C.; Zhang, X.; Zhou, M.; He, S.; Gan, M.; Yang, L.; Wang, K. Impacts of urbanization and landscape pattern on habitat quality using OLS and GWR models in Hangzhou, China. *Ecol. Indic.* **2020**, *117*, 106654. [[CrossRef](#)]
12. Xu, H. A remote sensing index for assessment of regional ecological changes. *China Environ. Sci.* **2013**, *33*, 889–897.
13. Zhang, Y.; She, J.; Long, X.; Zhang, M. Spatio-temporal evolution and driving factors of eco-environmental quality based on RSEI in Chang-Zhu-Tan metropolitan circle, central China. *Ecol. Indic.* **2022**, *144*, 109436. [[CrossRef](#)]
14. Yuan, B.; Fu, L.; Zou, Y.; Zhang, S.; Chen, X.; Li, F.; Deng, Z.; Xie, Y. Spatiotemporal change detection of ecological quality and the associated affecting factors in Dongting Lake Basin, based on RSEI. *J. Clean. Prod.* **2021**, *302*, 126995. [[CrossRef](#)]
15. Geng, J.; Yu, K.; Xie, Z.; Zhao, G.; Ai, J.; Yang, L.; Yang, H.; Liu, J. Analysis of spatiotemporal variation and drivers of ecological quality in Fuzhou based on RSEI. *Remote Sens.* **2022**, *14*, 4900. [[CrossRef](#)]
16. An, M.; Xie, P.; He, W.; Wang, B.; Huang, J.; Khanal, R. Spatiotemporal change of ecologic environment quality and human interaction factors in three gorges ecologic economic corridor, based on RSEI. *Ecol. Indic.* **2022**, *141*, 109090. [[CrossRef](#)]
17. Xu, H.; Wang, Y.; Guan, H.; Shi, T.; Hu, X. Detecting ecological changes with a remote sensing based ecological index (RSEI) produced time series and change vector analysis. *Remote Sens.* **2019**, *11*, 2345. [[CrossRef](#)]
18. Chen, Y.; Yang, J.; Yang, R.; Xiao, X.; Xia, J.C. Contribution of urban functional zones to the spatial distribution of urban thermal environment. *Build. Environ.* **2022**, *216*, 109000. [[CrossRef](#)]
19. Yao, L.; Wei, W.; Yu, Y.; Xiao, J.; Chen, L. Rainfall-runoff risk characteristics of urban function zones in Beijing using the SCS-CN model. *J. Geogr. Sci.* **2018**, *28*, 656–668. [[CrossRef](#)]
20. Zheng, Y.; Du, S.; Zhang, X.; Bai, L.; Wang, H. Estimating carbon emissions in urban functional zones using multi-source data: A case study in Beijing. *Build. Environ.* **2022**, *212*, 108804. [[CrossRef](#)]
21. Guo, S.; Li, Y.; He, P.; Chen, H.; Meng, J. Embodied energy use of China's megacities: A comparative study of Beijing and Shanghai. *Energy Policy* **2021**, *155*, 112243. [[CrossRef](#)]
22. Cao, J.; Law, S.H.; Samad, A.R.B.A.; Mohamad, W.N.B.W.; Wang, J.; Yang, X. Effect of financial development and technological innovation on green growth—Analysis based on spatial Durbin model. *J. Clean. Prod.* **2022**, *365*, 132865. [[CrossRef](#)]
23. Gong, P.; Chen, B.; Li, X.; Liu, H.; Wang, J.; Bai, Y.; Chen, J.; Chen, X.; Fang, L.; Feng, S.; et al. Mapping essential urban land use categories in China (EULUC-China): Preliminary results for 2018. *Sci. Bull.* **2020**, *65*, 182–187. [[CrossRef](#)] [[PubMed](#)]
24. Chen, Z.; Chen, J.; Zhou, C.; Li, Y. An ecological assessment process based on integrated remote sensing model: A case from Kaikukang-Walagan District, Greater Khingan Range, China. *Ecol. Inform.* **2022**, *70*, 101699. [[CrossRef](#)]
25. Nedkov, R. Orthogonal transformation of segmented images from the satellite Sentinel-2. *Cr. Acad. Bulg. Sci.* **2017**, *70*, 687–692.
26. Peng, X.; Wu, W.; Zheng, Y.; Sun, J.; Hu, T.; Wang, P. Correlation analysis of land surface temperature and topographic elements in Hangzhou, China. *Sci. Rep.* **2020**, *10*, 10451. [[CrossRef](#)]
27. Wu, P.; Zhong, K.; Wang, L.; Xu, J.; Liang, Y.; Hu, H.; Wang, Y.; Le, J. Influence of underlying surface change caused by urban renewal on land surface temperatures in Central Guangzhou. *Build. Environ.* **2022**, *215*, 108985. [[CrossRef](#)]
28. Zhou, S.; Liu, D.; Zhu, M.; Tang, W.; Chi, Q.; Ye, S.; Xu, S.; Cui, Y. Temporal and Spatial Variation of Land Surface Temperature and Its Driving Factors in Zhengzhou City in China from 2005 to 2020. *Remote Sens.* **2022**, *14*, 4281. [[CrossRef](#)]
29. Song, C.; Yang, J.; Wu, F.; Xiao, X.; Xia, J.; Li, X. Response characteristics and influencing factors of carbon emissions and land surface temperature in Guangdong Province, China. *Urban. Clim.* **2022**, *46*, 101330. [[CrossRef](#)]
30. Liu, W.; Meng, Q.; Allam, M.; Zhang, L.; Hu, D.; Menenti, M. Driving factors of land surface temperature in urban agglomerations: A case study in the pearl river delta, china. *Remote Sens.* **2021**, *13*, 2858. [[CrossRef](#)]
31. Wang, J.; Xu, C. Geodetector: Principle and prospective. *Acta Geographica Sinica* **2017**, *72*, 116–134.
32. Wang, J.; Hu, Y. Environmental health risk detection with GeogDetector. *Environ. Modell. Softw.* **2012**, *33*, 114–115. [[CrossRef](#)]
33. Luo, X.; Yang, J.; Sun, W.; He, B. Suitability of human settlements in mountainous areas from the perspective of ventilation: A case study of the main urban area of Chongqing. *J. Clean. Prod.* **2021**, *310*, 127467. [[CrossRef](#)]
34. Zhao, Z.; He, B.; Li, L.; Wang, H.; Darko, A. Profile and concentric zonal analysis of relationships between land use/land cover and land surface temperature: Case study of Shenyang, China. *Energy Build.* **2017**, *155*, 282–295. [[CrossRef](#)]
35. Ren, J.; Yang, J.; Wu, F.; Sun, W.; Xiao, X.; Xia, J. Regional thermal environment changes: Integration of satellite data and land use/land cover. *iScience* **2023**, *26*, 105820. [[CrossRef](#)]

36. Yang, J.; Xin, J.; Zhang, Y.; Xiao, X.; Xia, J. Contributions of sea–land breeze and local climate zones to daytime and nighttime heat island intensity. *NPJ Urban Sustain.* **2022**, *2*, 12. [[CrossRef](#)]
37. Yang, J.; Wang, Y.; Xue, B.; Li, Y.; Xiao, X.; Xia, J.; He, B. Contribution of urban ventilation to the thermal environment and urban energy demand: Different climate background perspectives. *Sci. Total Environ.* **2021**, *795*, 148791. [[CrossRef](#)] [[PubMed](#)]
38. Cui, R.; Han, J.; Hu, Z. Assessment of Spatial Temporal Changes of Ecological Environment Quality: A Case Study in Huaibei City, China. *Land* **2022**, *11*, 944. [[CrossRef](#)]
39. Ji, J.; Wang, S.; Zhou, Y.; Liu, W.; Wang, L. Spatiotemporal change and landscape pattern variation of eco-environmental quality in Jing-Jin-Ji urban agglomeration from 2001 to 2015. *IEEE Access.* **2020**, *8*, 125534–125548. [[CrossRef](#)]
40. Zhang, J.; Yang, G.; Yang, L.; Li, Z.; Gao, M.; Yu, C.; Gong, E.; Long, H.; Hu, H. Dynamic Monitoring of Environmental Quality in the Loess Plateau from 2000 to 2020 Using the Google Earth Engine Platform and the Remote Sensing Ecological Index. *Remote Sens.* **2022**, *14*, 5094. [[CrossRef](#)]
41. Huang, H.; Chen, W.; Zhang, Y.; Qiao, L.; Du, Y. Analysis of ecological quality in Lhasa Metropolitan Area during 1990–2017 based on remote sensing and Google Earth Engine platform. *J. Geog. Sci.* **2021**, *31*, 265–280. [[CrossRef](#)]
42. Aizizi, Y.; Kasimu, A.; Liang, H.; Zhang, X.; Zhao, Y.; Wei, B. Evaluation of ecological space and ecological quality changes in urban agglomeration on the northern slope of the Tianshan Mountains. *Ecol. Indic.* **2023**, *146*, 109896. [[CrossRef](#)]

**Disclaimer/Publisher’s Note:** The statements, opinions and data contained in all publications are solely those of the individual author(s) and contributor(s) and not of MDPI and/or the editor(s). MDPI and/or the editor(s) disclaim responsibility for any injury to people or property resulting from any ideas, methods, instructions or products referred to in the content.